Design of a Simple and Modular 2-DOF Ankle Physiotherapy Device Relying on a Hybrid Serial-Parallel Robotic Architecture

Christos E. Syrseloudis[a*], Ioannis Z. Emiris[a], Theodore Lilas[b], and Artemis Maglara[a,c]

[a] *Department of Informatics and Telecommunications, University of Athens, Athens, Greece*
[b] *Department of Shipping Trade and Transport, University of the Aegean, Chios, Greece*
[c] *Reflexion LTD, Piraeus, Greece*

(Received 20 November 2009; final version received ….)

The aim of this work is to propose a new 2-DOF robotic platform with hybrid parallel-serial structure and to undertake its parametric design so that it can follow the whole range of ankle related foot movements. This robot can serve as a human ankle rehabilitation device. The existing ankle rehabilitation devices present typically one or more of the following shortcomings: redundancy, large size, or high cost, hence the need for a device that could offer simplicity, modularity, and low cost of construction and maintenance. In addition, our targeted device must be safe during operation, disallow undesirable movements of the foot, while adaptable to any human foot. Our detailed study of foot kinematics has led us to a new hybrid architecture, which strikes a balance among all aforementioned goals. It consists of a passive serial kinematics chain with two adjustable screws so that the axes of the chain match the two main ankle-axes of typical feet. An active parallel chain, which consists of two prismatic actuators, provides the movement of the platform. Thus, the platform can follow the foot movements, thanks to the passive chain, and also possesses the advantages of parallel robots, including rigidity, high stiffness and force capabilities. The lack of redundancy yields a simpler device with lower size and cost. The paper describes the kinematics modelling of the platform and analyses the force and velocity transmission. The parametric design of the platform is carried out; our simulations confirm the platform's rightness for ankle rehabilitation.

Keywords: ankle rehabilitation, serial robot, parallel robot, design, kinematics, simulation.

1. Introduction

Typically, people with kinetic problems are required to work with a physiotherapist for a number of sessions. Ankle injuries are one of the most common phenomena. The aim of this work is to propose a new 2-DOF robotic platform with hybrid parallel-serial structure, to serve as a human ankle rehabilitation device. The existing ankle rehabilitation devices present typically one or more of the following shortcomings: redundancy, large size, heavy weight, or high cost, hence the need for a device that could offer simplicity, modularity, and low cost of construction and maintenance.

Simple rehabilitation devices, found in almost every physiotherapist clinic, are meant for functional rehabilitation. Such devices are elastic bands, foam rollers and wobble boards (PerformBetter). Elastic bands are the simplest devices, each made of multi-shaped strips of elastic. Foam rollers act as unstable surfaces and are used to improve balance and proprioception (one's inner perception of own body status). Wobble boards are circular discs with a hemispherical pivot in the center of one of the sides (Mattacola and Dwyer, 2002) (Figure 1). Unfortunately, these devices have several shortcomings.

Moving and exercising in the clinic is problematic for patients with serious injuries or patients in remote rural areas. Home exercising usually involves simple mechanical devices loaned to patients by clinics. These devices lack quantitative diagnostic and networking capabilities that would allow therapists to remotely monitor

* Corresponding author. Email:c.sirsel@di.uoa.gr

the patient's progress. Also they are rarely interactive, making exercising repetitive and boring, since the patient must perform repeatable and identical motions for a long time. This is also a repetitive, boring and time consuming task for the physiotherapist. In addition none of the existing simple devices cover all requirements of the rehabilitation tasks.

As a result, the interest for an automatic mechanical device that would provide physiotherapy exercises is significant and is actually increasing. Robotics offers

Figure 1. A wobble-board rehabilitation exercise (Mattacola and Dwyer, 2002).

powerful and secure methods for designing devices for physiotherapy exercises adapted to ankle injuries. Possessing tele-operation capabilities and remote data recording will be useful to patients that have severe injuries and cannot easily move, or live in remote rural areas.

1.1. Previous Work

There have been a number of robotic devices proposed for ankle physiotherapy. Important work has been carried out at Rutgers University by M. Girone et al. (2001) with the development of a haptic interface for human ankle rehabilitation (Figure 2). This haptic interface has been based on a 6-DOF Stewart platform that applies variable forces and virtual reality exercises on the patient's foot, including remote control operation. It has been tested successfully in orthopaedic rehabilitation, post-stroke rehabilitation, and rehabilitation of musculo-skeletal injuries.

However the Stewart platform has certain disadvantages. It is redundant for this application, since the ankle has fewer degrees of freedom (Dul and Johnson, 1985; Bogert et al. 1994). Also, the actuators used are noisy, the controller is oversized and the cost of the device is consequently high. In addition, in the rehabilitation program, there is no reference as to what extent the special characteristics of each patient's foot can be considered.

The work of J.S Dai et al. (2004) is based on the study of ankle injuries, and ankle functional anatomy, which is represented in an orientation image space. A particular area of this orientation space is selected to generate a desirable orientation range of motion for ankle rehabilitation. Three parallel tripod-type ankle rehabilitation mechanisms were proposed and their mobility and constraints were analyzed.

Figure 2. The Rutgers Ankle haptic interface (Girone et al. 2001).

The stiffness analysis and mechanism synthesis stemming from ankle physiotherapy motion led to a robotic device for sprained ankle rehabilitation. These are three or four actuator platforms and therefore they are redundant. Also, the rotation of the moving platform is performed about a vertical pivot strut, which is not a desirable characteristic for foot movements.

J. Yoon and J. Ryu (2005) proposed an ankle rehabilitation device based on a reconfigurable parallel robot. It is a 4-DOF

parallel robot with two moving platforms. It enables all desired ankle and foot motions, including toe and heel raising as well as the traditional ankle rotations. This is because the mechanism can generate the relative rotation between the front and the rear platforms as well as pitch and roll motions. To perform each mode of range of motion, strengthening, and proprioception exercises, a unified position-based impedance control is developed taking into account the desired position and velocity. However, this platform is quite complex and heavy and as a result is rather difficult in construction and transfer.

Recently, a 2-DOF redundantly actuated parallel mechanism for ankle rehabilitation was proposed by J.A. Saglia et al. (2009). The mechanism has the advantage of mechanical and kinematics simplicity when compared to existing multi-degree of freedom parallel mechanism prototypes, while at the same time it is fully capable of carrying out the exercises required in ankle rehabilitation protocols. The proposed device allows plantar / dorsiflexion and inversion / eversion using actuation redundancy to eliminate singularity, and to improve the workspace dexterity. However, this device is over-actuated, which means that there are redundant actuators. This also increases significantly the cost.

Syrseloudis, Emiris et al. (2008) analyzed the motions of the foot according to the 2-axes ankle model (Dul and Johnson, 1985) as well as the shape of the workspace which it covers. Experiments on the foot motions of several healthy human subjects were carried out by the use of a Mephisto 3D scanner and an MTi motion sensor of the XSens Motion Technologies. The workspace that the feet covers, as well as the forces (Maganaris et al. 2001), velocities and accelerations that it achieves when it moves over the entire allowed regions have been studied in detail.

A parallel Tripod (3-RPS) (Lee and Shah, 1988) with an extra rotation axis on the moving platform as a possible ankle rehabilitation device was studied by Syrseloudis and Emiris (2008) (Figure 3).

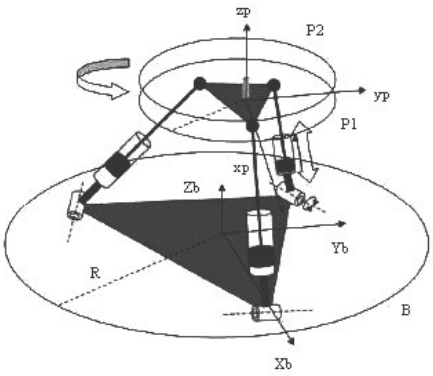

Figure 3. Tripod based ankle rehabilitation device.

The Tripod has two rotational (pitch, roll) and one translational (z) degrees of freedom. As the yaw angle changes significantly during the foot movements on the platform, an extra rotation axis was added on the moving platform to provide the necessary extra yaw angle, since the Tripod's original yaw is negligible. Although this device can follow the foot movements very satisfactorily, it is not simple enough for our purposes, hence our effort to design a robot with fewer DOFs.

There are more general devices offering rehabilitation. One example is by the TELEDOC project (Armada 2003), where they developed a complete computerised home rehabilitation system for the upper arm. Lastly, Toth and Ermolaev (2006) have used standard, full scale industrial serial robots for the physiotherapy of spastic hemiparetic stroke patients. Culmer et al. (2003) proposed a 3-DOF serial robot and a dual serial robot for the rehabilitation of the upper limb. This robotic structure is irregular and its stiffness capabilities are insufficient for the foot.

1.2. Our Contribution

Existing robotic mechanisms for ankle rehabilitation are typically redundant, oversized, too heavy, or quite expensive. This paper addresses the need for a design emphasizing the following features:

- adaptability to all human feet,
- simplicity, including a limited number of actuators leading to a smaller size and weight, low cost of construction and maintenance,
- mechanical adaptability and modularity for easy disassembling and transferring,
- safety, especially with respect to prohibited movements that can cause injuries to the human user.

For the rehabilitation task, the patient needs to sit on a bench while his shank is vertically fixed. Therefore, the foot must move while exercising only the ankle. The rehabilitation robot should be able to perform delicate motions so that it will not hurt the patient. However occasional load from the patient, like in the case of stepping onto the device, can exert much more load than the limiting forces. Therefore an over-design is required for the robot actuators which should be combined with additional safety force sensors in order to achieve safe operation. This issue would make a common serial robot unsuitable for the required operation and would make a parallel robot oversized.

Based on the biomechanics literature, in particular the description of the kinematics structure of the ankle, we adopted the standard 2-axes ankle model (Dul and Johnson, 1985), therefore leading us to a 2-DOF design. To fully respect the kinematics structure of the ankle, and obtain a simple device with two DOFs, we should add modularity via some mechanically adjustable capabilities.

These requirements led us to a new architecture of a hybrid serial-parallel robotic platform that can apply ankle rehabilitation exercises while respecting the aforementioned features. The robotic device is composed of a passive serial kinematics chain with two adjustable lengths and two prismatic actuators, which work in parallel, providing the necessary movements to the platform. The structure of the robot has been based on our study of foot kinematics as described in Syrseloudis, Emiris et al. (2008). Our objective was that the moving platform follows precisely the allowable movements of the foot without redundant characteristics. This is achieved with the assistance of two screws and in this way the device becomes mechanically adaptive to the two main ankle axes. This mechanical enhancement led to the elimination of additional actuators.

The proposed design decomposes the serial and parallel robots phenomena in a way that the passive mechanical structure accepts the high loads and the actuators are matched only for the patient exercise. Previous designs trying to decompose the above issues use a spherical joint (Dai et al. 2004). This approach decouples accidental forces from treatment torques hence a new problem arises. The machine axes of rotation are offset from the ankle axes of rotation therefore causing undesired movements to the patient. In the proposed design we manage to decouple accidental forces from treatment torque; we also match patients ankle rotation axes. Therefore treatment suitable devices can be a six degree Stewart platform and the proposed hybrid serial parallel design. Load comparison on actuators shows the benefits of our design namely: intrinsically safe operation, smaller actuators and two instead of six actuators. This leads to reduced cost, weight and also to simplicity. Compared to a possible software adjustment for the Stewart platform, the main difference of our hybrid design is the manual adjustments by the therapist, before patient treatment. Thus our design is safer because avoids wrong software input parameters.

Our 2-DOF hybrid robotic device possesses the minimal number of actuators and small controller size, consequently decreasing the construction cost. The passive serial chain allows the parallel actuators to work almost exactly like the two DOFs of the human foot; it is possible to adapt to any patient's foot mechanically before the session starts. Hence there is no need of very sophisticated task planning software and control during operation. This device is more secure, for example than a Stewart platform, because the Stewart platform may perform non-allowable movements. Lastly, the

proposed device can be easily transported and can operate at a remote-rural area.

The main objective of this paper is the parametric design of the new robotic platform which is based on the analysis and resulting specifications from Syrseloudis, Emiris et al. (2008), while additional measurements of specific points that define the two ankle axes of several feet have been carried out. These are used for the definition of the bounds of the two adjustable lengths of the robot. The robot has been, finally, simulated in MATLAB, where its kinematics behavior is graphically represented, thus confirming its usefulness in rehabilitation.

This paper has the following structure: first the kinematics of the foot is briefly introduced and Section 2. In Section 3, the architecture and the kinematics of the new hybrid serial-parallel robotic platform is analyzed and in Section 4, the parametric design of the platform is carried out. In Section 5 specific motions of the platform are graphically represented via simulations. We conclude with the suitability of the proposed architecture as an ankle rehabilitation device.

2. Foot kinematics

The structure and kinematics of the human foot are described in this section. The human ankle has a complex multi-joint structure (Dul and Johnson, 1985; Bogert et al. 1994). The central bone is the talus. Its surrounding bones are the calcaneus, the navicular and the cuboid; they are responsible The upper part of the talus articulates with the shank segment through the tibia and fibula bones. This is the upper ankle joint (denoted UAJ). It supports the rotational dorsiflexion / plantarflexion motion. The movements between the fore bones are strictly coupled for the rotation of the ankle joint in 3-dimensional space.

Motion of the foot with respect to the talus is regarded as a rotation about the (fixed) subtalar joint (denoted STJ); this supports the rotation called inversion / eversion. The main rotations of the foot are depicted in Figure 4 and the two axes of the ankle in Figure 5.

The UAJ is assumed to pass through the points P_3 (lateral malleolus) and P_4 (medial malleolus) while the STJ passes through the P_6 (calcaneus point) and P_7 (navicular point), see Figure 5 (Dul and Johnson, 1985). The lower limb is assumed to be composed of 3 rigid links capable to rotate between each other: the shank, the talus and the foot configuring a serial manipulator described in Dul and Johnson (1985) and in Syrseloudis, Emiris et al. (2008). The size of the foot bones, their relative positions as well as the orientation of the rotation axes, jointly determine the foot kinematics. Many factors influence the joint rotation, e.g. the shape of the articular surfaces, and the position of rotation axes. Constraint and resistance on the foot motions are due to ligaments, capsules and tendons.

A serial manipulator equivalent to the foot is obtained as follows. The shank-link connects the center K_1 of the P_1P_2 segment and the center K_2 of the P_3P_4 segment. The talus-link connects the center K_2 of the P_3P_4 segment and the center K_3 of the P_6P_7 segment.

Finally, the foot-link connects the center K_3 of the P_6P_7 segment with point P_8, which is on the fifth metatarsal. The knee-axis

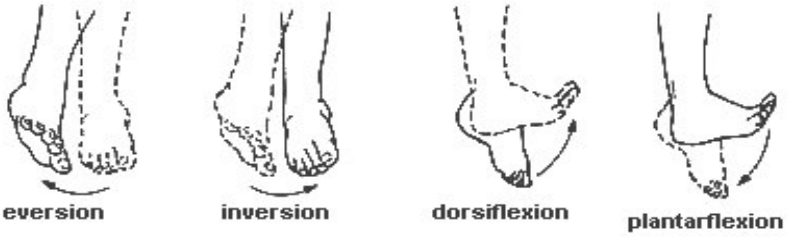

Figure 4. Main rotations of the foot about the two axes of the ankle.

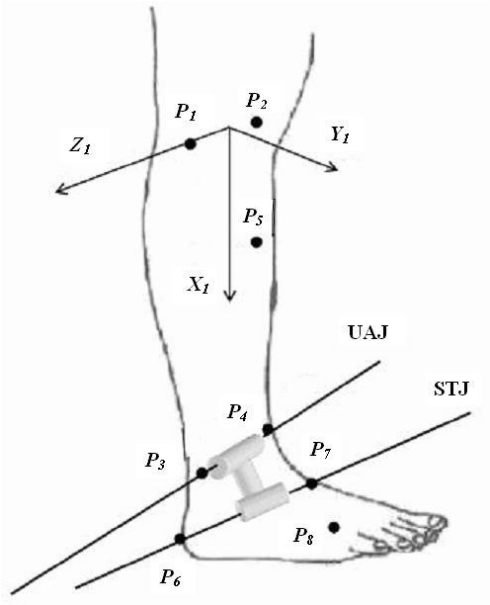

Figure 5. Main rotation axes of the ankle.

which is defined by P_1-P_2, is assumed to be fixed. The rotational Upper Ankle Axis and the Subtalar Axis are defined by the P_3-P_4 and P_6-P_7 axes, respectively. The main rotations of the foot about the ankle are defined according to the right-hand rule in Figure 6. In particular, plantarflexion is the negative and dorsiflexion is the positive rotation around the UAJ (Z_2) axis. Similarly, inversion is the negative and eversion is the positive rotation around the STJ (Z_3) axis.

The foot kinematics can be approximated by terms of serial manipulator kinematics. We use homogeneous matrix transformations according to the Denavit-Hartenberg notation, denoted DH (Denavit and Hartenberg, 1955). The assigned relative frames O_i between the moving links are shown in Figure 6. T_i^{i+1} is the transformation matrix from O_{i+1} into O_i defined as follows:

$$T_i^{i+1} = \begin{bmatrix} c(\theta_i) & -c(\alpha_i)s(\theta_i) & s(\alpha_i)s(\theta_i) & a_i c(\theta_i) \\ s(\theta_i) & c(\alpha_i)c(\theta_i) & -s(\alpha_i)c(\theta_i) & a_i s(\theta_i) \\ 0 & s(\vartheta_i) & c(\vartheta_i) & d_i \\ 0 & 0 & 0 & 1 \end{bmatrix} \quad (1)$$

where c(*)=cos(*), s(*)=sin(*) and i=1,…,4.

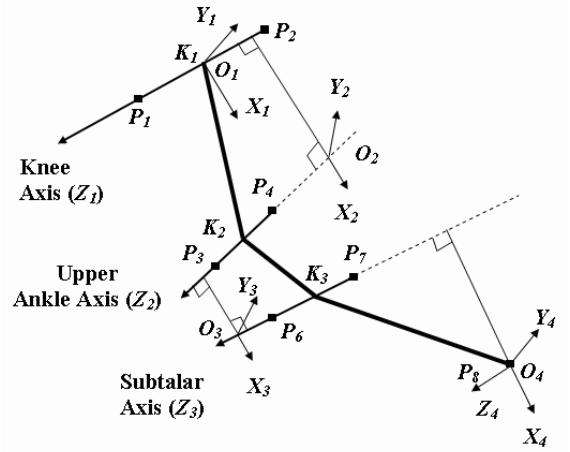

Figure 6. Serial kinematics chain of the foot and D-H frames assignment.

The transformation matrix from the last into the first coordinate system is given by the relation:

$$T_1^4 = T_1^2 T_2^3 T_3^4 . \quad (2)$$

The last coordinate system is that of the foot, system $O_4X_4Y_4Z_4$ on Figure 6. For a point $P = [x \ y \ z \ 1]^T$ on this system, the above transformation into the first (shank) coordinate system can be expressed as $P_{o1} = [x_1 \ y_1 \ z_1 \ 1]^T$ where

$$P_{o1} = T_1^4 P . \quad (3)$$

These equations give a parametric formula of the D-H parameters in the movement of P with respect to the fixed coordinate system of the shank. The D-H parameters are defined as follows, by referring to Figure 6:

- α_i is the twist angle between the Z_i, Z_{i-1} axes,
- a_i is the length of the common normal to the Z_i, Z_{i-1} axes,
- d_i is the offset between the common normals a_i and a_{i-1} ,
- θ_i is the rotation angle between X_i, X_{i-1}.

The independent variables of the model are the angles θ_2 (dorsiflexion / plantarflexion), and θ_3 (inversion / eversion), whereas θ_1 is constant. The zero configuration of the equivalent serial manipulator is taken to be when the foot is in the erect standing pose. The values of the variable angles about the zero configuration are taken to lie in the following ranges: $-40^o \le \theta_2 \le 25^o$ and $-20^o \le \theta_3 \le 20^o$ (Nigg et al., 1992; Syrseloudis et al., 2008). This analysis concerns the right leg while movements of the left leg are assumed to be the mirror-image of the right leg (Dul and Johnson, 1985). The parameters α_i, a_i, d_i depend on the foot anatomy and size.

In Dul and Johnson (1985) the transformation matrices expressed in Euler angles were estimated for a male subject. Standard instruments were used to measure the distances between the bony landmarks. After the calculation of several internal distances using the triangulation technique, the redundant distance method was used for the calculation of the transformation matrices between the foot and the talus, and between the talus and the shank frames. From these data, a kinematics model of the foot was based on homogeneous matrix transformations in Euler angles. We used the Maple computer algebra software (version 9.5) to perform (partly symbolic) calculations on the distances, and obtained the desirable D-H parameters (Syrseloudis, Emiris et al. 2008).

Taking into account the previously mentioned motions, it might seem conceivable that a serial robot would be able to meet the requirements (Culmer et al. 2003; Toth and Ermolaev 2006). However, industrial serial robots are huge and a 3-DOF serial robot with structure similar to that of the foot, and having a platform-shape end-effector, has some serious drawbacks. The size of the serial chain must be quite small and actuators should be mounted on the joints. This makes the robotic structure irregular with insufficient stiffness capabilities.

To overcome this problem, we propose a 2-DOF parallel robot with a passive serial kinematics chain, which constraints the movements (Figure 7) and a parallel chain, which provides the movements. The objective is to incorporate the advantages of parallel robots as they have rigidity, high manipulability and heavy loads handling.

3. A 2-DOF ankle rehabilitation platform

This section discusses the proposed hybrid serial-parallel robotic architecture and its kinematics characteristics.

The robot consists of a base platform and a moving platform like most parallel robots. The latter is where the patient's foot shall be placed. A vertical strut connects the base of the robot with a passive serial chain. The serial chain has structure similar to that of the foot and provides the necessary constraints on the movements. It has one revolute and one cylindrical joint which support the rotations about the two main rotation axes of the ankle, see Figure 7. R_1 is a revolute-joint which is collinear with the Upper Ankle Joint (UAJ) and C_2 is a cylindrical-joint which is collinear with the Subtalar Joint (STJ) of the foot. The serial chain is connected with the moving platform and has two adjustable screws so that the corresponding lengths D_1, D_2 can be adjusted according to the axes position of each individual patient's foot. The parallel chain consists of two prismatic actuators which are connected with the moving platform through

S-Joints (points A_1, A_2) and with the base platform through U-Joints (points B_1, B_2).

3.1. Kinematics modeling of the platform

We start by modeling the kinematics of our device. The mobility of the platform is modeled by applying the Grübler formula for spatial structures (Merlet 2006). The total number of its degrees of freedom N is given as follows:

$$N = 6(n - j - 1) + \sum f_i = 6\ (8\text{-}9\text{-}1) + 14 = 2\ . \quad (4)$$

where n represents the total number of rigid bodies of the mechanism, including the base, j is the total number of joints, and f_i the number of degrees of freedom of joint i. Of course the summation is understood over all joints.

Initially we assign the base coordinate frame $O_bx_by_bz_b$ on the fixed base and the moving frame $O_px_py_pz_p$ on the moving platform as shown in Figure 7. The two frames are parallel when the moving platform is in zero position. As we have a serial kinematics chain it is useful to implement the Denavit-Hartenberg method (Denavit and Hartenberg, 1955) for the assignment of the relative reference frames on the passive serial chain and therefore to obtain the overall kinematics formula of the platform, see Equation (1).

The $O_ox_oy_oz_o$ frame is the base frame of the serial chain and is placed arbitrarily on the strut with the axis z_o collinear with the UAJ axis, and x_o collinear with z_b, as shown in Figure 7. The origin O_2 of the $O_2x_2y_2z_2$ frame is the O_p of the platform frame and the axis z_2 is parallel with z_1 (C_1).The total transformation matrix T is given by the multiplication:

$$T = T_b T_0^1 T_1^2 T_r\ . \quad (5)$$

where T_b is a constant homogeneous rotation matrix defining the relative rotation of the $O_ox_oy_oz_o$ frame into the base $O_bx_by_bz_b$ frame. The points on the platform coordinate frame need to be multiplied with an extra rotation matrix T_r in order to be transformed into the last D-H frame of the serial chain. The D-H parameters can be computed on the host computer in which the orientation and position of the two axes of rotation are given as inputs. Consequently the inverse kinematics problem is described from the following two equations:

It is well known that the Jacobian matrix is a key part for the study and design of robots. It appears in the equations which describe the relation between the velocities, accelerations and forces of the end-effector and the actuated joints. Furthermore, it is used for the allocation of singular configurations. In our case, the velocities of the actuators and the moving platform are connected through the equation:

$$\begin{bmatrix} \dot{L}_1 \\ \dot{L}_2 \end{bmatrix} = J^{-1}\begin{bmatrix} v_x & v_y & v_z & \omega_x & \omega_y & \omega_z \end{bmatrix}^T . \quad (8)$$

where J^{-1} is a 2x6 pose-dependent inverse Jacobian matrix, v_x, v_y, v_z are the linear velocities and ω_x, ω_y, ω_z the angular velocities of the end-effector. By following the normalized Plücker vector-based procedure for the inverse Jacobian calculation of a general parallel robot as it is described in detail in Merlet, (2006) we get:

$$J^{-1} = \begin{bmatrix} n_1 & n_1 \times A_1O_p \\ n_2 & n_2 \times A_2O_p \end{bmatrix}. \quad (9)$$

where n_1, n_2 are the unit vectors of B_1A_1, B_2A_2.

$$L_1^{\,2} = \|B_1A_1\|_2 = \|T \cdot A_1 - B_1\|_2\ , \quad (6)$$

$$L_2^{\,2} = \|B_2A_2\|_2 = \|T \cdot A_2 - B_2\|_2\ . \quad (7)$$

where L_1, L_2 are the length of the actuated links.

3.2. Velocity and Force Transmission

When the linear actuators are activated their velocities and applying forces are transferred onto the moving platform. The relations between the forces-velocities of the actuators and the moving platform are expressed by the Jacobian matrix and are pose-dependent. The wrench force vector F and the actuator force vector τ are related in the following way:

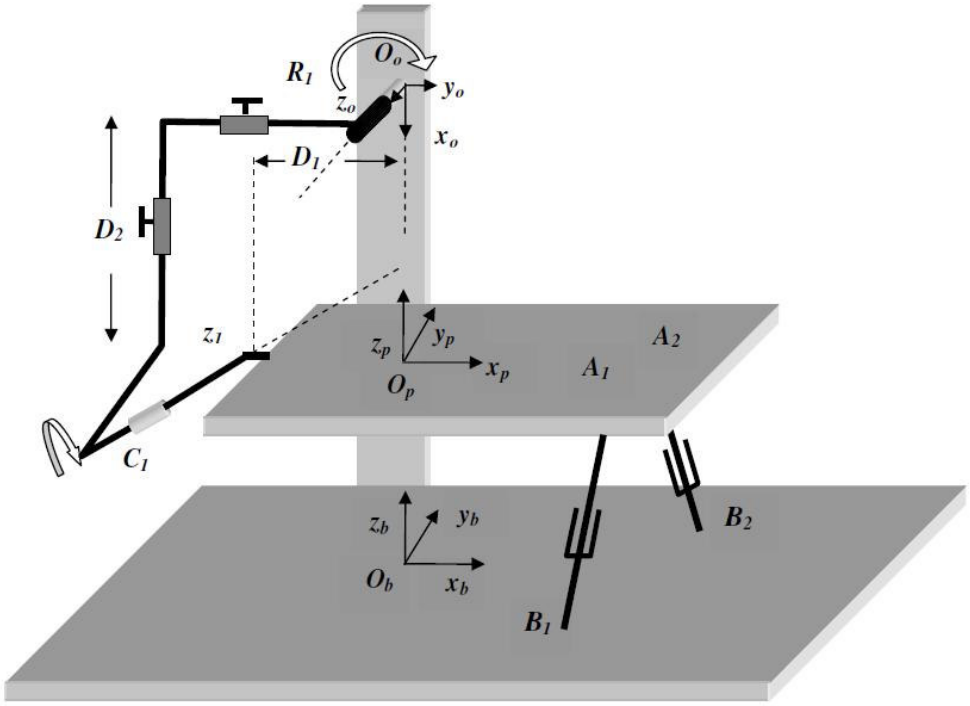

Figure 7. The 2-DOF hybrid parallel-serial robotic platform for ankle rehabilitation.

$$F = J^{-T}\tau . \qquad (10)$$

Also the relation between the linear velocities $\dot{L}$ of the actuators and the vector of linear and angular velocities $\dot{X}$ of the moving platform is:

$$\dot{L} = J^{-1}\dot{X} . \qquad (11)$$

Given the desired velocities as well as the force and moments that should be handled by the platform, the extreme values of the velocities and forces of the linear actuators are computed in the design phase. Here we follow the kinetostatic capability analysis of a parallel manipulators described in Kim and Choi (1999) where the calculation of the magnitude bounds of the force and velocities of the end-effector is reduced to an eigenvalue problem. Matrix M is essential here and is defined as follows:

$$M = J^{-T} J^{-1} = \begin{bmatrix} A & B \\ B^T & C \end{bmatrix}. \qquad (12)$$

The linear forces and torques have different units it is reasonable for the bounds computation of force-torques at the end-effector to be decoupled into two constraint maximization subproblems, one for the forces f and one for the torques m. By use of matrix M the two maximization subproblems can be rearranged into the following eigenvalue subproblems:

$$A \cdot f = a_f^{\,2} \cdot f\,, \qquad (13)$$

$$C \cdot m = a_m^{\,2} \cdot m\,. \qquad (14)$$

where A, C are the 3×3 submatrices of M and f, m the 3×1 vectors of linear forces and torques on the end-effector. By Equation (13), a three-dimensional force transmission ellipsoid is defined which has principal axes given by f and radii given by a_f. In the same way, Equation (14) defines a torque transmission ellipsoid with principal axes defined by m, and radii defined by a_m. The bounds of force and torques magnitudes are now given by the inequalities:

$$\frac{\|f\|}{a_{f\max}} \le \|\tau\| \le \frac{\|f\|}{a_{f\min}}\,, \qquad (15)$$

$$\frac{\|m\|}{a_{m\max}} \le \|\tau\| \le \frac{\|m\|}{a_{m\min}}\,. \qquad (16)$$

where $\|\,.\,\|$ is the Euclidean norm, a_{fmax} and a_{fmin} denote the square roots of the maximum and minimum eigenvalues of A, and a_{mmax} and a_{mmin} are those of the maximum and minimum eigenvalues of C. In the above, τ is the 2×1 forces vector applied by the linear actuators.

Following a similar procedure as in the force transmission analysis, velocity transmission analysis is decoupled in two subproblems, one for the linear v and one for the angular ω velocities magnitudes.

$$A \cdot v = a_v^{\,2} \cdot v\,, \qquad (17)$$

$$C \cdot \omega = a_\omega^{\,2} \cdot \omega\,. \qquad (18)$$

where A, C are the 3×3 submatrices of M and v, ω the 3×1 vectors of linear and angular velocities of the end-effector. The bounds of the velocities magnitudes are therefore given from the inequalities

$$a_{v\min}\|v\| \le \left\|\dot{L}\right\| \le a_{v\max}\|v\|\,, \qquad (19)$$

$$a_{\omega\min}\|\omega\| \le \left\|\dot{L}\right\| \le a_{\omega\max}\|\omega\|\,. \qquad (20)$$

where a_{vmax} and a_{vmin} denote the square roots of the maximum and minimum eigenvalues of A, and $a_{\omega max}$ and $a_{\omega min}$ are those of the maximum and minimum eigenvalues of C. $\dot{L}$ is the 2×1 vector of linear velocities applied by the actuators. Matrix M is pose dependent and concerns one specific configuration. By discretizing the whole workspace of the robot and computing the global extreme eigenvalues of M, the global magnitude bounds of velocities and forces are computed.

4. Parametric Design of the Robot

This section presents the parametric design of our mechanism, since we have chosen the robotic architecture.

Design concerns the calculation of the geometric parameters of the robot satisfying our requirements (Merlet 1995, 2006). These requirements are, for example, the workspace covered by the end-effector, the desired velocities and accelerations, and the specification of the force capabilities for load handling.

Based on the above foot analysis, the following values were selected for initial dimensioning of the device:

- Moving platform: 0.40x0.20m so that it can accept all or at least the majority of human foot sizes.
- Base platform: 0.60x0.40m. The first axis z_o is placed 50cm above the fixed base.

The bounds of rotation axes of the serial chain were defined according to the range of the feet rotations described in Nigg et al. (1992) and Syrseloudis, Emiris et al. (2008) and so they are: $-40^{o} \le z_o \le 20^{o}$, and $-20^{o} \le z_1 \le 20^{o}$. The STJ axis, and so the z_1 has the mean foot orientation as it is given in Isman and Inman (1969) and forms an angle of 23^{o} with the $x_p z_p$ plane and an angle of 41^{o} with the $x_p y_p$ plane.

The design of the platform was based on the design framework described in Syrseloudis, Emiris et al. (2008). This work has been extended and in order to complete the design of the robot, additional measurements on the foot of several human subjects have been conducted. Coordinates of specific points of the foot, shown in Figure 5, have been measured, utilizing a Microscribe coordinate measuring device (Figure 8) (Microscribe 3D Digitizer). For the experimental measurements the right feet of 19 adult males and females have been used in the erect standing pose.

The UAJ is defined by points P_3 (lateral malleolus) and P_4 (medial malleolus), while the STJ is defined by points P_6 (calcaneus point) and P_7 (navicular point) (Figure 5). For calculating the bounds on distance D_1 the points P_3, P_4 and P_6 were

Figure 8. The Microscribe 3-dimensional coordinate measurement device.

projected on the horizontal plane. The vertical distance of the projected point P_6 from the projected line P_3P_4 defines distance D_1. The computed values of D_1 were found to be in the range:

$$0.035\text{m} \le D_1 \le 0.056\text{m}. \qquad (21)$$

with mean value 0.0483m and standard deviation 0.0068m. For calculating the range of distance D_2, the mean value of the height of points P_3 and P_4 from the horizontal plane was computed. The resulting values are in the following range:

$$0.054\text{m} \le D_2 \le 0.093\text{m}. \qquad (22)$$

with mean value 0.0729m and standard deviation 0.0102m. Figure 9 depicts graphically the values of the computed distances D_1, D_2 per human subject.

Points A1, A2 on the moving platform have been assigned coordinates (0.15,-0.06,0) and (0.15,0.06,0) of the moving frame,

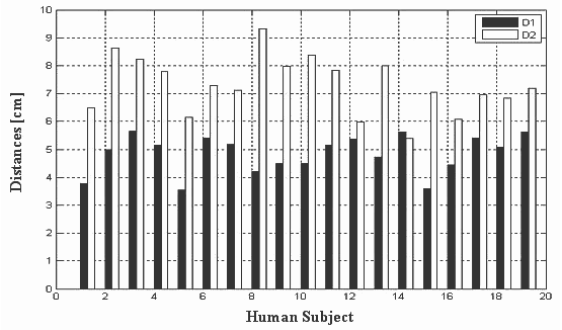

Figure 9. Foot distances D_1 (black bars), and D_2 (white bars), measured for 19 human subjects.

respectively. If the points are far from the rotation axis then the actuators apply smaller forces but larger velocities. Reversely, if the points are near the rotation axis then the actuators apply forces with larger values and smaller velocities. Therefore, the points are selected to be in the middle of the platform in order to balance the amounts of the velocities and forces exerted by the actuators. The coordinates of the base platform points B1, B2 have been assigned to (0.10,-0.15,0) and (0.10,0.15,0) respectively, on the base reference frame nearer to the origin so to avoid singularities. The coordinate units are in m. When the platform moves through the entire range of rotations and parameters D_1, D_2 take all values in the above intervals, then

the length of the legs are found in the range: [0.31m, 0.56m].

Having computed the kinematics parameters of the robot as well as the desired end-effector velocities and wrench forces, the actuator velocities and forces can be computed. The values of these parameters are transferred to the platform and depend on the geometric characteristics of the platform through the inverse Jacobian. The platform must handle torque values up to 200Nm as described in Syrseloudis, Emiris et al. (2008). The result is coming from Maganaris et al. (2001) in which they studied the tension torque that the soleus and tibialis anterior muscles can exert. These are two of the main dorsiflexor-plantaflexor muscles and the maximum measured torque was about 121Nm. Also they state that in Fukunaga et al. (1996) the maximum measured torques of the whole plantarflexor and dorsiflexor muscle groups were about 143Nm. Therefore a desired upper bound of 200Nm includes a wide range of foot torque capabilities. In order for the platform to achieve these torque bounds, the actuator forces must be greater than 675N according to Equation (16).

Similarly, for velocities calculation used the upper bounds in angular velocities of the platform studied in Syrseloudis, Emiris et al. (2008). An MTi motion sensor was used for the measurement of the foot angular velocities among several human subjects. The MTi sensor was fastened on the sole of the foot under the ankle and angular velocity in the following three movements were measured: dorsiflexion / plantarflexion, inversion / eversion and full rotations of the foot. The maximum recorded angular velocity was 9.3rad/sec and therefore the upper bound of 10 rad/sec is adopted. According to Equation (20), the linear actuators should achieve velocities at least 2.1m/sec in order to reach the bound of 10rad/sec.

Now the design of the robot is completed and from the dimensioning of the robot its individual parts can be mechanically designed and prepared. Also from the actuators force-velocity bounds the motor characteristics providing the robot motion can be selected.

5. Design evaluation of the robot

This section evaluates the design of the proposed device. In order to study the robot better and for visualization purposes, a simulation has been developed in a Matlab GUI. The workspace shows that the platform movements match with the workspace of the foot because rotates about the two main rotation axes of the ankle and therefore the resulting movements are in agreement with that of the foot. The platform in two different poses is depicted in Figure 10.
depicted in Figure 13. The units of the vector are the same as before. It is obvious that the resulting torques are smaller than 200Nm satisfying the design requirements.

For the study of the velocity transmission of the robot, the platform was rotated with the maximum angular velocity of 10rad/sec performing a pure dorsiflexion. The linear velocities of the actuators with respect to the dorsiflexion angle are graphically calculated (Equation 11) in Figure 14(a-b) respectively. Actuator 1 refers to B_1A_1 and actuator 2 refers to B_2A_2.

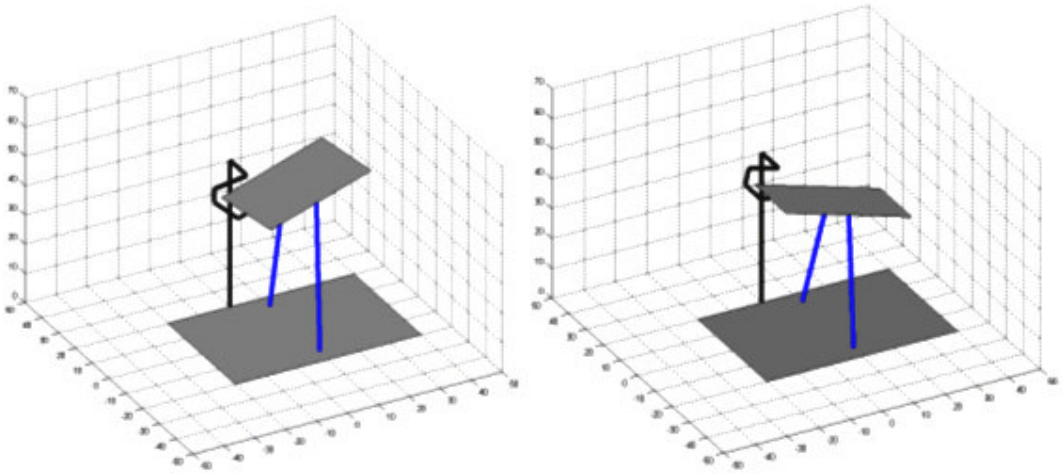

Figure 10. The robotic platform in 2 different poses.

Next, the force transmission from the actuators to the moving platform was graphically represented according to Equation 10. We assumed that the linear actuators apply the maximum linear forces of 675N producing a pure dorsiflexion rotation. The torque vector of the moving platform with respect to the dorsiflexion angle is depicted in Figure 12, while the units of the torques are in Nm.

In the second step, we assumed that the linear actuators apply the maximum linear forces of 675N performing a pure eversion rotation. The torque vector of the moving platform with respect to the eversion angle is

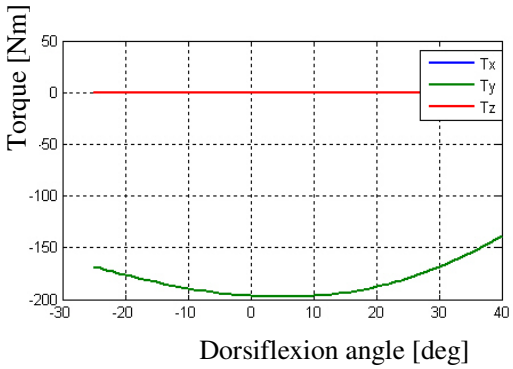

Figure 12. Platform torques in a pure dorsiflexion rotation.

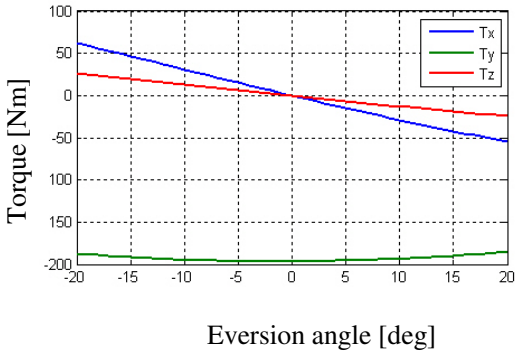

Figure 13. Platform torques in a pure eversion rotation.

Similarly the platform was assumed to rotate with the same maximum angular velocity, but in a pure eversion rotation. The corresponding linear velocities of the actuators with respect to the eversion angle are now depicted in Figure 15(a-b). Linear velocities are expressed in m/sec and angular velocities in rad/sec. It is clear that the resulting velocities are smaller than the required 2.1m/sec

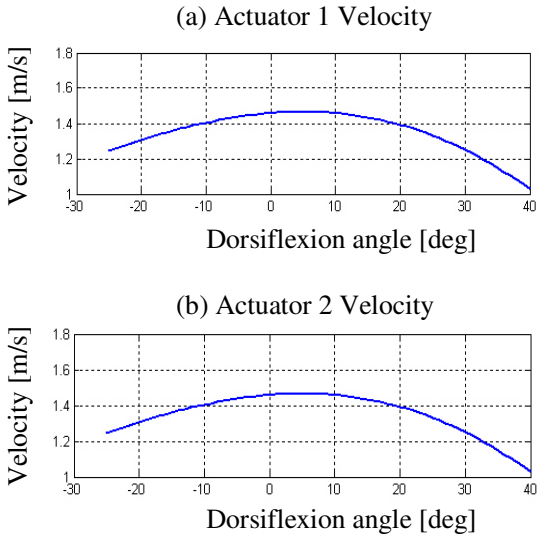

Figure 14. Actuators velocity in a pure dorsiflexion rotation.

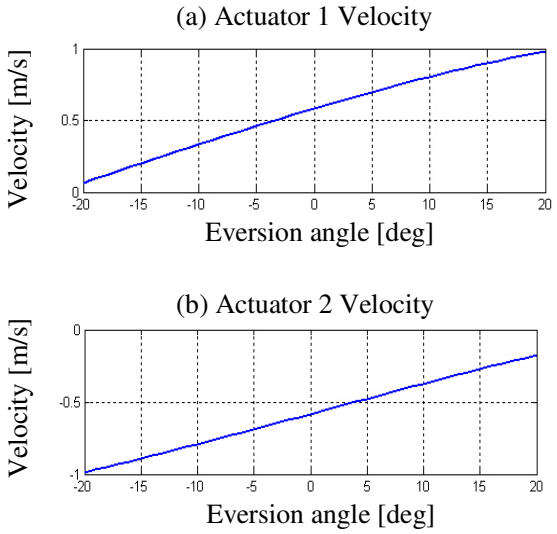

Figure 15. Actuators velocity in a pure eversion rotation.

The simulation show that the robot can follow the movements of the foot about the two main axes of the ankle. Finally, the graphically representation of force-torques and velocities values of the robot are found to lie within the bounds specified by the design requirements, evaluating the design of section 4.

6. Conclusion

Let us conclude with a summary of results and future work.

In this paper a new 2-DOF hybrid serial-parallel robot was presented. The proposed robotic device can follow the movements of the foot with respect to the ankle and, consequently, can be used as a rehabilitation device for ankle injuries treatment. The structure of the robotic platform has been decided after the detailed study of foot kinematics. The main objective was to overcome the drawbacks of the existing devices which are typically redundant, oversized, heavy, or expensive.

The resulting robotic structure is a platform with the minimal number of actuators so as to minimize the size and cost. The hybrid serial-parallel design allows the parallel actuators to work almost exactly like the 2 DOF's of the human foot. The addition of two extra adjustable screws enable the platform to be adjusted according to the characteristics of each individual patient's foot. The adjustment is performed prior to the rehabilitation session.

The above result in the following advantages: the task planning software and the kinematics control during operation are simplified. The device is considerably safer in comparison to a redundant platform because, in the latter case, the second platform may perform a non-allowed movement. Finally, design of the platform has been carried out according to the foot motions requirements.

In the future, the mechanical design of the proposed robotic platform will be performed. Extensive stiffness analysis according to finite element analysis (e.g ANSYS software package) or virtual joint method (VJM) (Pashkevich et al. 2009) will be implemented for the study of the robot's behavior in loading conditions. This analysis is necessary for the kind and thickness of materials which will be used, mainly for the strut and the passive serial chain which sustains the main torque amounts. Also, the serial kinematics chain can become more easily adjustable to the kinematics characteristics of typical feet. The dynamic modeling of the platform is also a subject for

research. Compliant control algorithms such as force control, impedance control etc, which are appropriate for the rehabilitation task, will be studied in detail based on special injury treatment. The construction of the platform and its use in rehabilitation exercises on actual patients is our final task.

In parallel, an identification method of foot kinematics parameters is being developed, which estimates the foot axes and kinematics parameters (Syrseloudis et al., 2009), by recording foot movements with a coordinate measuring device, and with no use of any internal angle measurement, extending the ideas from (Daney and Emiris, 2001). Identification of the ankle axes and foot kinematics parameters is useful in the rehabilitation exercise. In this way, a general device (e.g. Stewart platform) can suitably perform the trajectory planning or a mechanically adjustable device can be tuned properly such as a future version of the robot proposed here with more adjustable parameters.

Finally, the simplicity of the described design makes it easy for our device to be enhanced with tele-operation capabilities and remote data recording in order to be useful to patients that cannot move, or live in remote areas.

Acknowledgments

The authors thank Dr. C.N. Maganaris (Manchester Metropolitan University) for his support in the study of ankle kinematics. The second author has carried out part of this work while on leave at the SALSA joint team of INRIA and Univ. de Paris VI. This work is supported by the General Secretariat of Research and Technology of Greece through a PENED 2003 program, contract Nr. 70/03/8473, co-funded by the European Social Fund (75%) and National resources (25%). The latter includes a contribution by private company Reflexion Ltd (10%).

References

ANSYS. http://www.ansys.com

Armada M. 2003. International Advanced Robotics Programme (IARP) 22nd JOINT COORDINATING FORUM Madrid, Report on Robotics Research in Spain. http://www.iai.csic.es/iarp/sapr/12_SPAIN_IARP_JCF_2003.pdf

Bogert AJ van den, Smith GD, Nigg BM. 1994. In Vivo Determination of the Anatomical Axes of the Ankle Joint Complex: An Optimization Approach. *J. Biomechanics*, Vol. 27, No. 12, pp. 1477-1488.

Culmer P, Jackson A Savage J, Levesley M, Richardson R,. Cozens A, Williams MM, Bhakta B,. 2003. From single to dual robotic therapy: A review of the development process of iPAM. *Biomed. Robotics & Biomechatronics*, pages 347–352.

Dai JS, Zhao T, Nester C. 2004. Sprained ankle physiotherapy based mechanism synthesis and stiffness analysis of a robotic rehabilitation device. *Autonomous Robots*, 16:207–218.

Denavit J, Hartenberg R. 1955. A kinematics notation for lower-pair mechanisms based on matrices. *J. Applied Mechanics*, pages 215–221.

Daney D, Emiris I. 2001. Robust parallel robot calibration with partial information. *Proc. IEEE Intern. Conf. Robotics & Automation,* pp.3262-3267, Seoul, Korea.

Dul J, Johnson GE. 1985. A kinematics model of the human ankle. *J. Biomedical Engineering*, 7:137–143.

Fukunaga T., Roy RR, Shellock FG, Hodgson JA, Edgerton VR. 1996. Specific tension of human plantarflexors and dorsiflexors. *J Applied Physiology*, 80:158–165.

Girone M, Burdea G, Bouzit M, Popescu V, Deutsch JE. 2001. A Stewart platform-based system for ankle telerehabilitation. *Autonomous Robots*, 10:203–212.

Isman RE, Inman VT. 1969. Anthropometric studies of the human foot and ankle. *Bulletin Prosthetic Research*, 10-11:97–129.

Kim HS., Choi YJ. 1999. The Kinetostatic Capability Analysis of Robotic Manipulators. *Proc. IEEE/RSJ Intern. Conf. Intelligent Robots and Systems*. Kyongju, Korea.

Lee K, Shah D.K. 1988. Kinematic Analysis of a three degrees of freedom in parallel actuated manipulator. *J. Robotics and Automation*, Vol 4(3) pages 354-60.

Maganaris CN, Baltzopoulos V, Ball D, and Sargeant AJ. 2001. In vivo specific tension of human skeletal muscle. *J. Appl. Physiol*., 90(3):865–72.

Mattacola CG, Dwyer MK. 2002. Rehabilitation of the Ankle After Acute Sprain or Chronic Instability. *J. Athletic Training*. 37(4). pp. 413-429.

Merlet J-P. 1995. Designing a parallel robot for a specific workspace. INRIA Sophia-Antipolis, France. Technical Report 2527.

Merlet J-P. 2006. *Parallel Robots*. Springer, The Netherlands, 2nd edition.

Microscribe 3D Digitizer. http://www.ghost3d.com/ gt_systems.htm.

Nigg BM, Fisher V, Allinger TL, Ronsky JR, Engsberg JR. 1992. Range of motion of the foot as a function of age. *Foot & Ankle*, 16(6):336–343.

Pashkevich A, Chablat D, Wenger P. 2009. Stiffness analysis of overconstrained parallel manipulators, *Mechanism and Machine Theory*. 44 pp. 966-982.

PerformBetter. http://www.performbetter.com.

Saglia J, Tsagarakis NG,. Dai JS, Caldwell DG. 2009. A High Performance 2-dof Over-Actuated Parallel Mechanism for Ankle Rehabilitation, *Proc. IEEE Intern. Conf. Robotics & Automation*, Kobe, Japan.

Syrseloudis C, Emiris I, Maganaris C, Lilas T. 2008. Design framework for a simple robotic ankle evaluation and rehabilitation device. *Proc. 30th IEEE Intern. Conf. Engineering in Medicine & Biology*, pages 1410–1413, Vancouver, Canada.

Syrseloudis C, Emiris I. 2008. A Parallel Robot for Ankle Rehabilitation: Evaluation and its Design Specifications. *8th IEEE Intern. Conf. Bioinformatics & Bioengineering*, pages 1-6, Athens, Greece.

Syrseloudis C, Emiris I, Daney D. 2009. Idenetification of Foot Kinematics Paramaters. Manuscript.

Toth A, Ermolaev I. 2006. Robots with patients. *Engineer IT*, pages 60–62.

Yoon J, Ryu J. 2005. A Novel Reconfigurable Ankle/Foot Rehabilitation Robot . *Proc. IEEE Intern. Conf. Robotics & Automation*. Barcelona, Spain.